# Improving the Performance of the Chaotic Nonlinear System of the Fractional-Order Brushless Direct Current Electric Motor by Using Fractional-Order Sliding Mode Control

**Amin Kaveh**
Islamic Azad University
**Mohammad Vahedi** (Mo.Vahedi@iau.ac.ir)
Islamic Azad University
**Majid Gandomkar**
Islamic Azad University

**Research Article**

**Keywords:** Brushless direct current electric motor, order-deficit, parameter changes, chaos, sliding-order-deficit mode control, Lyapunov stability

**Posted Date:** July 18th, 2023

**DOI:** https://doi.org/10.21203/rs.3.rs-3166378/v1



**Additional Declarations:** No competing interests reported.

# Improving the Performance of the Chaotic Nonlinear System of the Fractional-Order Brushless Direct Current Electric Motor by Using Fractional-Order Sliding Mode Control

**Amin Kaveh[1], Mohammad Vahedi [2,*] and Majid Gandomkar [1]**

[1] Department of Electrical Engineering, College of Technical, Islamic Azad University, Iran
[2] Department of Mechanical Engineering, College of Technical, Islamic Azad University, Iran (corresponding author)

**Abstract**

Chaos is a dynamic phenomenon that occurs over time in discrete and continuous nonlinear systems for some parameters, and chaotic systems are very sensitive to initial conditions. Controlling a chaotic system means eliminating its chaotic behavior and bringing the system to its origin equilibrium point or another desirable point. Moreover, as most natural systems have fractional dynamics, there is a clear need to study fractional systems. Nowadays, Brushless Direct Current (BLDC) electric motors are widely used as actuator components in many industries. Controlling these nonlinear and multivariable systems is of great importance. Additionally, these systems are often accompanied by parameter uncertainties and external disturbances, which may lead to undesirable and even unstable system behavior. In this research, a three-state-variable chaotic model is presented, and with the help of fractional-order sliding mode control strategy, the performance of the system is improved and controlled compared to conventional sliding mode control. It can be seen that the resistance of the fractional-order BLDC system with fractional-order sliding mode control is significantly higher than that of the conventional BLDC system with conventional sliding mode control against parameter uncertainties and external disturbances. Finally, the controller's performance is evaluated using MATLAB software.

**Keywords:** Brushless direct current electric motor, order-deficit, parameter changes, chaos, sliding-order-deficit mode control, Lyapunov stability.

## 1. Introduction

Nowadays, vehicles are increasingly being equipped with PM synchronous motors. One of the types of motors that is of interest is the brushless DC motor, which is considered a permanent option in large industries such as automotive due to its sensorless operation nature. These motors provide maximum torque at standstill, and this torque decreases linearly with increasing speed. However, due to the square wave shape of the current and the commutation action between the phases, they have a certain amount of ripple torque, which can affect their performance. This article examines various methods that have been developed to reduce torque ripple in these motors [1-4].

By examining the performance of various motors used today, it can be concluded that conventional DC motors have high efficiency despite their need for a commutator and brush, which requires special care. To address this issue, a special type of motor called the brushless DC (BLDC) motor has been proposed. The BLDC motor is a permanent magnet motor with a rotor made of permanent magnet and a stator winding similar to normal motors. Unlike conventional DC motors, a brush is not needed for commutation in BLDC motors, which is instead done by electronic devices. These motors can have one or two poles, and the inverter plays the role of commutator during operation [1-4].

The BLDC motor has several technical advantages over conventional and induction DC motors. These advantages include simplicity of the control system and minimal need for sensors, long life and low maintenance, appropriate torque-speed characteristic, good dynamic response, high efficiency, noiseless operation, high speed range, and high ratio of produced torque to engine volume. Overall, these benefits make the BLDC motor a popular choice in many industries, particularly in applications where high efficiency, low noise, and precise control are required. Based on the features mentioned above, it is reasonable to use the BLDC motor in applications that require high power and torque and have space limitations. The motor's compact size, high efficiency, and appropriate torque-speed characteristic make it a suitable option for such applications. In a novel sensorless control scheme for the interior permanent magnet synchronous motor (IPMSM) drive system to achieve high-performance speed control. The proposed approach utilizes a terminal sliding mode observer to replace the real mechanical sensor and obtain the rotor position and speed information, ensuring observer stability[5].

Fractional calculus is being increasingly applied in various fields. This mathematical concept allows for a more accurate description and modeling of real systems, which are typically fractional in nature [6]. One of the most important areas of application for fractional calculus is in chaos theory. Chaotic systems are highly sensitive to initial conditions, and chaotic behavior occurs when phase plane trajectories of the system are globally bounded but locally unstable. It is currently known that chaos does not occur in non-linear continuous-time systems with an order less than three. The model of a chaotic system is typically represented by three separate differential equations that include order-fractional derivatives [7]. Shaoling Li Et al present a solution to the problem of increased bridge current distortion and power loss in modular multilevel converters (MMC) due to circulating current. The proposed solution is a circulating current controller based on fractional order differential sign function sliding modecontrol (FO-SMC). The controller incorporates fractional order calculus into the sign function to improve the response speed of the system while reducing chattering.[8]

The existence of chaos in motor systems was first discovered by Kuroe in 1989 [9,10]. A mathematical model for a permanent magnet synchronous motor was developed for the first time to analyze chaos and bifurcation [11]. In recent years, the use of BLDC motors has expanded greatly in the automotive, aerospace, household appliances, robotics, food and chemical industries, electric vehicles, medical devices, and computer peripherals [12,13]. Due to their high efficiency, long lifespan, low noise, and good speed-torque characteristics, BLDC motors have received significant attention [14]. The chaotic behavior of the BLDC motor system was found by Hemati in 1994 [15]. In most engineering applications, the occurrence of chaos in motors is highly undesirable for their performance [9]. Therefore, studies on chaos control in BLDC systems have been conducted [16,17]. Synchronization of chaotic BLDC systems has also been studied [18]. The presence of chaos in BLDC motors leads to system oscillations, acoustic noise, mechanical vibration, and increased electrical energy consumption, which reduces the motor's lifespan. Therefore, studying chaos in the system can help improve the motor's design and prevent its occurrence [19-21].

Since the 1970s, the dynamic characteristics of various electric motors have been extensively studied for startup issues, speed control, and oscillations. Studying the dynamic characteristics of motors presents several challenges, such as their low-speed characteristics, which are notorious for low-frequency oscillations in controlled speed motors. These problems are closely related to studies on chaos in nonlinear systems. It is evident that the existing mathematical models for multi-variable BLDC motors are highly nonlinear and strongly coupled, which can exhibit complex behaviors. The BLDC electric motor is a highly efficient and powerful type of motor. With the development of permanent magnetic materials, its unique advantage has become increasingly apparent, and it is widely used in various motor-driven systems, servo systems, and household appliances [9].

The objective of this article is to design a fractional order sliding mode controller for controlling a chaotic behavior in a brushless direct current (BLDC) motor system. For this purpose, a desired control input sliding surface is designed by selecting an appropriate sliding level, which results in controlling the chaotic behavior and making the system's behavior smoother, reducing its vibration modes. Additionally, this design leads to better adaptation of the control system and increases its resistance to external disturbances and uncertainties.

## 2. Fractional order chaotic BLDC electric motor

In this section, the dynamic characteristics of a brushless direct current electric motor (BLDC) are studied. First, the mathematical model of the system is extracted, which is suitable for investigating bifurcation and chaos analysis. Then, the equilibrium points of the system and their types will be obtained.

### 2.1. Brushless DC electric motor system

As depicted in Figure 1, a brushless DC electric motor (BLDC) is powered by a DC electric power source[22]. Unlike traditional DC motors, a BLDC motor uses a closed-loop electronic controller to convert the incoming DC current into motor coils that generate magnetic fields. This enables the motor to rotate automatically in space without the need for brushes. The electronic controller also ensures precise control over rotation speed and direction. The phase and amplitude controller adjusts the DC current pulses to control the motor's speed and torque. Many conventional electric motors use a mechanical commutator (brush), but brushless motors offer many advantages over brushed DC motors. These advantages include a high torque-to-weight ratio, increased efficiency, more torque output per watt, increased reliability, reduced noise, longer life by eliminating erosion of the brush and commutator, and the removal of ionizing sparks from the commutator, resulting in an overall reduction of

electromagnetic interference. In converting electricity to mechanical power, brushless motors are more efficient than brushed motors, mainly due to the absence of brushes, which reduces the loss of mechanical energy due to friction. This leads to higher efficiency in the no-load and low-load regions of the motor performance curve [23, 24].

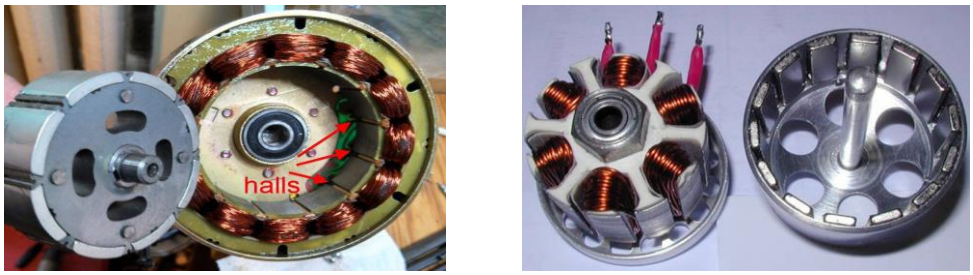


**Fig 1.** Schematic of a BLDC motor [21]

### 2.2. Problem statement

The dynamic equations of a BLDC electric motor are given in the following [23, 24]:

$$\begin{cases} \dfrac{di_d}{dt} = \dfrac{1}{L_d}\left[v_d - R\, i_d + \omega L_q i_q\right] \\ \dfrac{di_q}{dt} = \dfrac{1}{L_d}\left[v_q - R\, i_q - \omega L_d i_d - \omega\, \psi_r\right] \\ \dfrac{d\omega}{dt} = \dfrac{1}{J}\left[n_p \psi_r i_q + n_p\left(L_d - L_q\right) i_d\, i_q - T_L - \beta\omega\right] \end{cases} \quad (1)$$

Where $(v_d, i_d)$ and $(v_q, i_q)$ are the d-q voltage and current of the electric motor, $L_q$ and $L_d$ are the stator inductances, and $R$ is the stator resistance. $\psi_r$, $\beta$, and $J$ are the fixed magnetic flux, friction coefficient, and polar moment of inertia. The number of pair of poles is represented by $n_p$. $T_L$ is the external load torque, and $\omega$ is the rotor angular velocity. Based on an agreement, system (1) is simplified using the following transformations [23]. Assuming $T = \begin{bmatrix} bk & 0 & 0 \\ 0 & k & 0 \\ 0 & 0 & R/L_q \end{bmatrix}$, where $b = L_q/L_d$ , $k = \frac{\beta R}{L_q n_q \psi_r}$. And $\gamma = \frac{\psi_r}{k L_q}$, $\sigma = \frac{\beta\, L_q}{R\, J}$, $u_d = \frac{v_d}{R\, k}$ , $u_q = \frac{v_q}{R\, k}$, $v = \frac{n_p b\, L_q^2 k^2 ((L_d - L_q))}{J\, R^2}$, $\widetilde{T_L} = \frac{L_q^2\, T_L}{J\, R^2}$, and $t' = (R\, t)/L_q$ and state variables are obtained as $(\widetilde{.}) = T^{-1}(.)$. Using these transformations, system (1) is obtained as the following set of dimensionless equations [23]:

$$\begin{cases} \dfrac{d\tilde{\imath}_d}{dt'} = u_d - \mu\, \tilde{\imath}_d + \tilde{\omega}\tilde{\imath}_q \\ \dfrac{d\tilde{\imath}_q}{dt'} = u_q - \tilde{\imath}_q - \tilde{\omega}\tilde{\imath}_d + \gamma\tilde{\omega} \\ \dfrac{d\tilde{\omega}}{dt} = \sigma\left[\tilde{\imath}_q\left(\tilde{\imath}_q - \tilde{\omega}\right) + \tilde{\imath}_d + v\, \tilde{\imath}_d\tilde{\imath}_q - \widetilde{T}_L\right] \end{cases} \quad (2)$$

Such that $\sigma, \gamma, \mu$ and $v$ are the structural parameters of the dynamic system of the motor after transformations. And are the d-q reference voltage and current of the electric motor, $\widetilde{T}_L$ is the load torque after transformation, and $\tilde{\omega}$ is the rotor angular velocity after transformation. Assuming $\tilde{\imath}_q = x_1$, $\tilde{\imath}_d = x_2$, $\tilde{\omega} = x_3$ similar to the Lorentz system, the dynamic equations of the BLDC system are converted to the state space form:

$$\begin{cases} \dot{x}_1 = -\mu x_1 + x_2 x_3 + u_d \\ \dot{x}_2 = -x_2 - x_1 x_3 + \gamma x_3 + u_q \\ \dot{x}_3 = -\sigma(x_3 - x_2) - \widetilde{T}_L + v\, x_1 x_2 \end{cases} \quad (3)$$

The fractional order form of such a system is as follows [25, 26]:

$$\begin{cases} {}_0D_t^{q_1} x_1 = -\mu x_1 + x_2 x_3 + u_d \\ {}_0D_t^{q_2} x_2 = -x_2 - x_1 x_3 + \mu x_3 + u_q \\ {}_0D_t^{q_3} x_3 = -\sigma(x_3 - x_2) - \widetilde{T}_L + v\, x_1 x_2 \end{cases} \quad (4)$$

It should be noted that considering fractional-order dynamics in many systems can improve stability or increase accuracy in system behavior. The numerical solution of the fractional-order BLDC system is given by the following equations [6,25]:

$$\begin{cases} x_1(t_k) = -\mu x_1(t_{k-1}) + x_2(t_{k-1})x_3(t_{k-1}) + \\ \qquad u_d(t_{k-1})h^{q_1} - \sum_{j=v}^{k} c_j^{(q_1)} x_1(t_{k-j}) \\ x_2(t_k) = -x_2(t_{k-1}) - x_1(t_k)x_3(t_{k-1}) + \\ \gamma\, x_3(t_{k-1}) + u_q(t_{k-1})h^{q_2} - \sum_{j=v}^{k} c_j^{(q_2)} x_2(t_{k-j}) \\ x_3(t_k) = \sigma\, x_2(t_k) - x_3(t_{k-1}) - \overline{T}_L(t_{k-1}) + \\ \qquad v\, x_1(t_k)\, x_2(t_k)h^{q_3} - \sum_{j=v}^{k} c_j^{(q_3)} x_3(t_{k-j}) \end{cases} \tag{5}$$

Where $T_{sim}$ is the simulation time, $N = [T_{sim}/h] \quad k = 1, 2, \dots, N$ and $(x_1(0),\ x_2(0), x_3(0),)$ are the initial conditions. Binomial coefficients, $c_j^{(q)}$, are obtained considering the recursive equation.

### 2.3. Equilibrium points of BLDC system

Since we are interested in the chaotic dynamics of the system, we need to focus on the equilibrium points and parameter ranges where we observe chaos.

In order to obtain the fixed points of the system (3), we examine it for $\mu = 1$ and $v = 0$ under no-load conditions ( $u_d = u_q = \overline{T}_L = 0$ ) [3, 9]:

$$\begin{cases} \dot{x}_1 = -x_1 + x_2x_3 \\ \dot{x}_2 = -x_2 - x_1x_3 + \gamma x_3 \\ \dot{x}_3 = -\sigma(x_3 - x_2) \end{cases} \tag{6}$$

Therefore, we have:

$$\dot{x}_1 = 0, \quad \begin{cases} x_1 = 0 \\ x_1 = x_2x_3 \end{cases} \tag{7}$$

$$\dot{x}_2 = 0, \quad \begin{cases} x_2 = 0 \\ x_2 = x_3(\gamma - x_1) \end{cases} \tag{8}$$

$$\dot{x}_3 = 0, \quad \begin{cases} x_3 = 0 \\ x_2 = x_3 \end{cases} \tag{9}$$

By solving equations (7) to (9), three fixed points are obtained. We derive these equilibrium points and discuss their local behavior.

### 2.4. Bifurcation and chaos in BLDC system

Hopf bifurcation occurs when the corresponding Jacobian matrix has a pair of pure imaginary poles, and other eigenvalues of the real part are non-zero. Here, for the BLDC system, the Hopf bifurcation and its chaotic behavior under no-load condition ( $u_d = u_q = \overline{T}_L = 0$ ) are investigated. By examining Eq. (7) to Eq. (9), it is clear that $E_1 = (0, 0, 0)$ is the first equilibrium point. And with $\gamma > 1$, two other nontrivial equilibria are $E_2 = (\gamma - 1, \sqrt{\gamma - 1},\ \sqrt{\gamma - 1})$ and $E_3 = (\gamma - 1, -\sqrt{\gamma - 1}, -\sqrt{\gamma - 1})$.

A simple analysis shows that if $0 < \gamma < 1$, the original equilibrium point is stable, and it loses its stability for $\gamma = 1$and creates two unreal equilibrium points that are initially stable. By linearizing the system, we obtain the Jacobian matrix to discuss the local behavior of its equilibrium points. The Jacobian matrix of the system is as follows [23]:

$$J = \begin{bmatrix} -1 & x_3 & x_2 \\ -x_3 & -1 & -x_1 + \gamma \\ 0 & \sigma & -\sigma \end{bmatrix} \tag{10}$$

which has eigenvalues obtained by the roots of the following equation:

$$D(\lambda) = \lambda^3 + (2 + \sigma)\lambda^2 + (\sigma + \gamma)\lambda + 2\sigma(\gamma - 1) = 0 \tag{11}$$

When checked at non-origin equilibrium points (nontrivial equilibria). Note that since the two nontrivial equilibria are symmetric, their stability must be the same. For the bifurcation of two nontrivial equilibria, that is, the parameter values for which $\lambda = 0$ or $\lambda = j\omega$, is the solution of Eq. (11). With $\lambda = 0$, we have $\gamma = 1$, which results in bifurcation that was discussed. With $\lambda = j\omega$ and setting the real and imaginary parts equal to each other, we have:

$$\begin{cases} -\omega^3 + (\sigma + \gamma)\omega = 0 \\ -(2+\sigma)\omega^2 + 2\sigma(\gamma - 1) = 0 \end{cases} \quad (12)$$

Where $\omega^2 = \frac{2\sigma(\gamma-1)}{2+\sigma} = \sigma + \gamma$ By sorting, the value of $\gamma$ at which Hopf bifurcation occurs is obtained.

For $\omega^2 > 0$ , at this value of $\gamma$, that is:

$$\gamma_h = \frac{\sigma(\sigma+4)}{\sigma-2} \quad (13)$$

Which holds always for $\sigma > 2$. Therefore, the eigenvalues would be:

$$\omega^2 = \frac{2\sigma(\sigma+1)}{\sigma-2} > 0 \quad (14)$$

Therefore, the eigenvalues will be as follows:

$$\lambda_1 = -(\sigma+2), \quad \lambda_{2,3} = \pm j\sqrt{\frac{2\sigma(\sigma+1)}{(\sigma-2)}} \quad (15)$$

Therefore, $\gamma = \gamma_h$ corresponds to an Hopf bifurcation point of the system, and for values close to $\gamma \neq \gamma_h$, the equilibria are surrounded by the limit cycle, and for $\gamma > \gamma_h$, all three equilibria would be unstable. System (6) does not change under $(x, y, z) \Leftrightarrow (x, -y, -z)$; thus, it can be said that it is symmetric regarding y and z axes and if $\nabla V = \frac{\partial}{\partial x}\left(\frac{dx}{dt}\right) + \frac{\partial}{\partial y}\left(\frac{dx}{dt}\right) + \frac{\partial}{\partial z}\left(\frac{dx}{dt}\right) = -(\sigma+2) < 0$, this system is convergent.

As mentioned before, if $\gamma \leq 1$, $E_1 = (0,0,0)$ is the only equilibrium point. When the system parameters change, we might expect BLDC to demonstrate stable, limit cycle, and chaotic behaviors.

## 3. The design of a control input for the fractional-order BLDC system.

### 3.1. The fractional-order BLDC system without control input

Firstly, we analyze the fractional-order BLDC system under the no-load condition ( $u_d = u_q = \widetilde{T}_L = 0$ ) and $v = 0$ in the form of equations (4). We represent the parameter vector as $(\mu, \gamma, \sigma) = (1,\ 20,\ 5.46)$ and consider the system in homogeneous orders as $q_1 = q_2 = q_3 = 0.995$ . To perform differentiation at the fractional order of 0.995, we can either first take the integral of the desired variable to the order of 0.005 and then take the first derivative of the result (Riemann-Liouville definition), or first take the first derivative of the function and then perform fractional-order integration of 0.005 (Caputo definition). If we do not apply any control input to the system $u(t) = 0$, it will exhibit chaotic behavior. For $T_{sim} = 50\ sec$, a constant time step of $h = 0.005$ , and initial conditions $(x_1(0), x_2(0), x_3(0)) = (0, 0, 0)$ the system will behave chaotically. With the above conditions, the state variables of the fractional-order BLDC system without a control signal are shown in Fig 2.

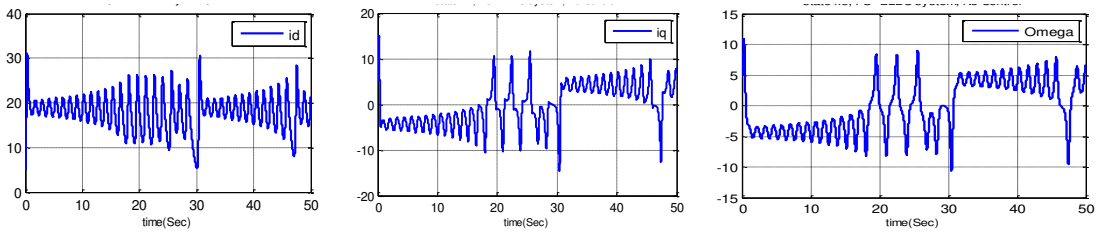


**Fig 2.** State variables $x_1(t)$, $x_2(t)$ and $x_3(t)$ of the fractional-order BLDC system without a control signal.

Furthermore, in Figs 3 and 4, the chaotic state trajectories of the fractional-order BLDC system without a control signal are also shown.

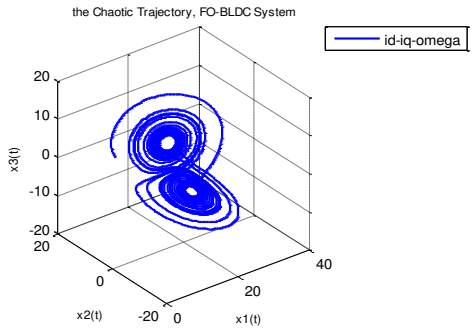


**Fig 3.** The chaotic state trajectories of the fractional-order BLDC system without a control signal are represented by $i_d$, $i_q$ and $\omega$

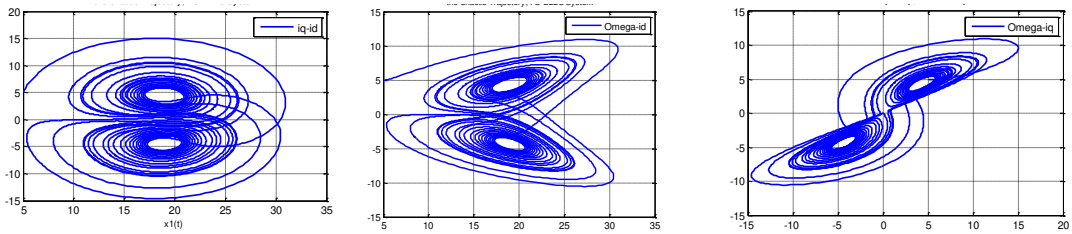


**Fig 4.** The chaotic state trajectories of the fractional-order BLDC system without a control signal are represented by $i_q - i_d$, $Omega - i_d$ and $Omega - i_q$

### 3.2. The fractional-order BLDC system with control input

3.2.1 Fractional-order sliding mode control

We know that the fractional-order equation is represented by the following relationship:

$$\begin{cases} {}_0D_t^{q_1}x_1 = -x_1 + x_2x_3 \\ {}_0D_t^{q_2}x_2 = -x_2 - x_1x_3 + \mu x_3 \\ {}_0D_t^{q_3}x_3 = -\sigma(x_3 - x_2) \end{cases} \quad (16)$$

According to the no-load conditions and the characteristics of section (3-1), using the trial and error method or drawing the bifurcation diagram, it can be seen that the system is unstable for $0 < q_1 = q_2 = q_3 = q < 0.6 \vee q > 1.1$ conditions and when $0.6 < q < 0.98$ converges to one of the two equilibrium points of $E_2 \vee E_3$ , and for $0.99 < q < 1.1$, chaotic behavior is generated. Therefore, to control this section, we consider the variable $q = 0.995$.

Considering that the controlled system is an order-fractional system, the desired sliding surface must also have an order-fractional form. We define the slip surface in such a way that $S \to 0$ equals to $x_2 \to 0$, therefore according to the order-fraction system of equations (16), we define the slip surface in the form of equation (17) [26]:

$$S = D_t^{q_2-1}x_2(t) \quad (17)$$

According to equation (17), if $x_2 \to 0$ equals $x_1 \to 0$ and $x_3 \to 0$, then the problem becomes a regulation problem.

3.2.2. Control input design

Next, the control input u is defined as follows [27-29]:

$$u = u_{eq} + u_N \quad (18)$$

As $u_{eq}$ is the equivalent control component and keeps the states on the sliding surface, and $u_N$ is the switching component and directs the states to the sliding surface, $u_N$ is actually responsible for stabilizing the system and uses the Lyapunov stability criterion.

$$\dot{S}(x) = \left[\frac{\partial S}{\partial X}\right]\dot{X}(t) = \quad (19)$$

$$\left[\frac{\partial S}{\partial X}\left(f(t,x) + B(t,x).(u_{eq} + u_N\right)\right] =$$

$$[\frac{\partial S}{\partial X}\big(f(t,x)+B(t,x).(u_{eq}+u_N)\big)]=$$
$$\Big[\frac{\partial S}{\partial X}\big(f(t,x)+B(t,x).u_{eq}\big)\Big]+\frac{\partial S}{\partial X}B(t,x)u_N=\frac{\partial S}{\partial X}B(t,x)u_N$$

If we assume that $\frac{\partial S}{\partial X}B(t,x)=I$ , where $I$ is the identity matrix, then we have $\dot{S}(x)=u_N$, which satisfies this condition sufficiently.

The condition for the existence of sliding mode ( condition $S_i\dot{S}_\iota<0$ ) is given by $S\neq 0$ . In the following, we will describe two important and commonly used cases in this article for the discontinuous control section:

a) Relay with constant gain:

$$u_{i_N}=\begin{cases}-\alpha_i Sign\big(S_i(x)\big) & S_i(x)\neq 0\ \ \alpha_i>0\\ 0 & S_i(x)=0\end{cases} \tag{20}$$

Where the $sign$ function is meant. If it is observed that by choosing this option for the discontinuous part of the control system, the above sufficient condition for sliding mode is satisfied, because:

$$S_i\dot{S}_i=-\alpha_i\,S_i(x)\,Sign\big(S_i(x)\big)<0 \qquad S_i(x)\neq 0 \tag{21}$$

b) Linear continuous feedback:

By choosing $u_{i_N}(x)=-\beta_i\,S_i(x)$ where $(\beta_i>0)$ as the discontinuous function, the sufficient condition for sliding mode according to the following equation is satisfied. In more general cases, the discontinuous part of the control system can be considered as a combination of the first and second cases.

$$S_i\dot{S}_i=-\beta_i\,S_i^2(x)<0 \tag{22}$$

c) Combination of Relay with Constant Gain and Linear Continuous Feedback

In general, the discontinuous control component can be considered as a combination of the first and second modes:

$$u_{i_N}=\begin{cases}-\alpha_i Sign\big(S_i(x)\big)-\beta_i\,S_i(x) & S_i(x)\neq 0\ \ \alpha_i<0\ \ \beta_i>0\\ 0 & S_i(x)=0\end{cases} \tag{23}$$

With this choice, the sufficient condition for the discontinuous part of the control is satisfied, because:

$$S_i\dot{S}_i=-\alpha_i S_i(x)Sign\big(S_i(x)\big)-\beta_i\,S_i^2(x)<0 \qquad S_i(x)\neq 0 \tag{24}$$

Now we denote the location of the control input in the fractional-order chaotic system:

$$\begin{cases} {}_0D_t^{q_1}x_1=-x_1+x_2x_3\\ {}_0D_t^{q_2}x_2=-x_2-x_1x_3+\gamma x_3+u(t)\\ {}_0D_t^{q_3}x_3=-\sigma(x_3-x_2)\end{cases} \tag{25}$$

which $u(t)$ is the same as the combined control input.

Since the sliding surface equation is defined based on the state variables according to equation (17), the system converges to the desired state on the sliding surface.

The following equations hold on the sliding surface:

$$\begin{cases}S=0\\ \dot{S}=0\end{cases} \tag{26}$$

To obtain the equivalent control law, it suffices to substitute $\dot{S}=0$:

$$\dot{S}={}_0D_t^{q_2}x_2=-x_2-x_1x_3+\gamma x_3+u_{eq}(t)=0 \tag{27}$$

The equivalent control law $u_{eq}(t)$ is obtained as follows:

$$u_{eq}(t)=-(-x_2-x_1x_3+\gamma x_3) \tag{28}$$

Now, considering the Lyapunov candidate function as a positive definite function, we have:

$$V=\frac{1}{2}S^2>0 \tag{29}$$

For asymptotic stability, the derivative of this function must be negative definite:

$$\dot{V}=S\,\dot{S}<0 \tag{30}$$

This is a proposed candidate for the switching control law to satisfy equation (30), and based on equation (21), it is given by:

$$u_N=-\beta\,Sign\big(S(x)\big)-\alpha\,S(x) \tag{31}$$

where $\alpha$ and $\beta$ are positive real values. By combining equations (28) and (30) and substituting into equation (18), the general sliding mode control law for regulating the state variables of a typical BLDC system is obtained:

$$u(t) = -(-x_2 - x_1 x_3 + \gamma x_3) - \beta\, Sign\big(S(x)\big) - \alpha\, S(x) \tag{32}$$

## 4. MATLAB software simulation

### 4.1. Fractional-order sliding mode control strategy

4.1.1. Phase and parametric diagrams in two states of uncontrolled and controlled.

Considering the parameter vector in the form of homogeneous orders $(\mu, \gamma, \sigma) = (1, 20, 5.46)$, we model the system as $q_1 = q_2 = q_3 = 0.995$ and $T_{sim} = 50\ sec$. We set the time constant $h = 0.005$ and initial conditions as $\big(x_1(0), x_2(0), x_3(0)\big) = (5, 5, 5)$. With the switching gain $k = 5$ and based on the sliding mode control input, we design relation (32) and implement it in MATLAB software. By plotting the phase trajectories $(\dot{x} - x)$ for the reference currents $(d - q)$ of the electric motor and the rotor angular speed $(\omega)$ in both uncontrolled and controlled states, we illustrate the system behavior in a single diagram. Similarly, we plot the previously separately plotted parametric diagrams for both uncontrolled and controlled states together [30].

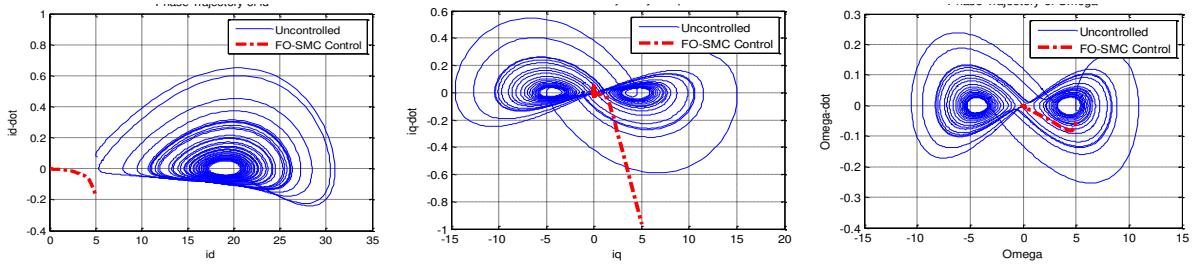


**Fig 5.** Phase plane diagram of state $x_1$, $x_2$ and $x_3$

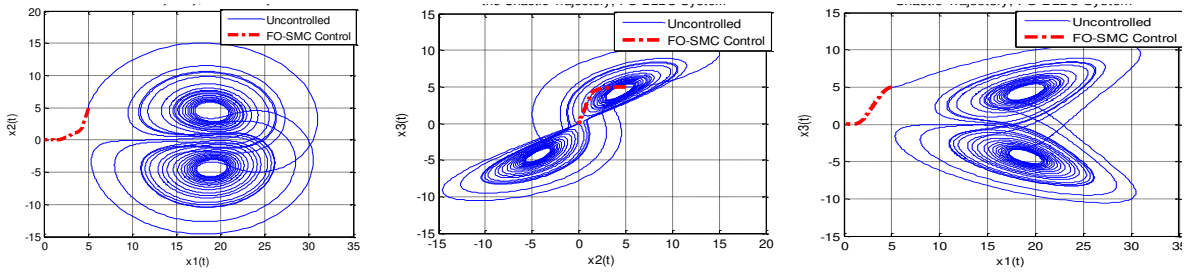


**Fig 6.** Parametric diagrams between state variables $x_1$ , $x_2$ and $x_3$ in uncontrolled and FO-SMC control

In all Figs 5 and 6, it is evident that the state variables and their rates of change have converged well to the zero set point. This indicates that the fractional-order sliding mode control has effectively regulated the state variables of the BLDC system to the desired zero set point.

4.1.2. Comparison of the designed fractional-order sliding mode control strategy with conventional sliding mode control:

Similar to before, we consider the system in the form of homogeneous orders with respect to the parameter vector $(\mu, \gamma, \sigma) = (1, 20, 5.46)$, we model the system as $q_1 = q_2 = q_3 = 0.995$ and $T_{sim} = 6\ sec$. The time constant is $h = 0.005$ and the initial conditions are defined as $\big(x_1(0), x_2(0), x_3(0)\big) = (5, 5, 5)$. With the switching gain $k = 5$, we design relation (32) based on the sliding mode control input using the signum function and implement it in MATLAB software to plot the state trajectories, rates of change of the states, control input, and sliding surface of the proposed method. We then compare the proposed method with conventional sliding mode control, which is applied to the system with the standard derivative, to determine the advantages of the proposed method.

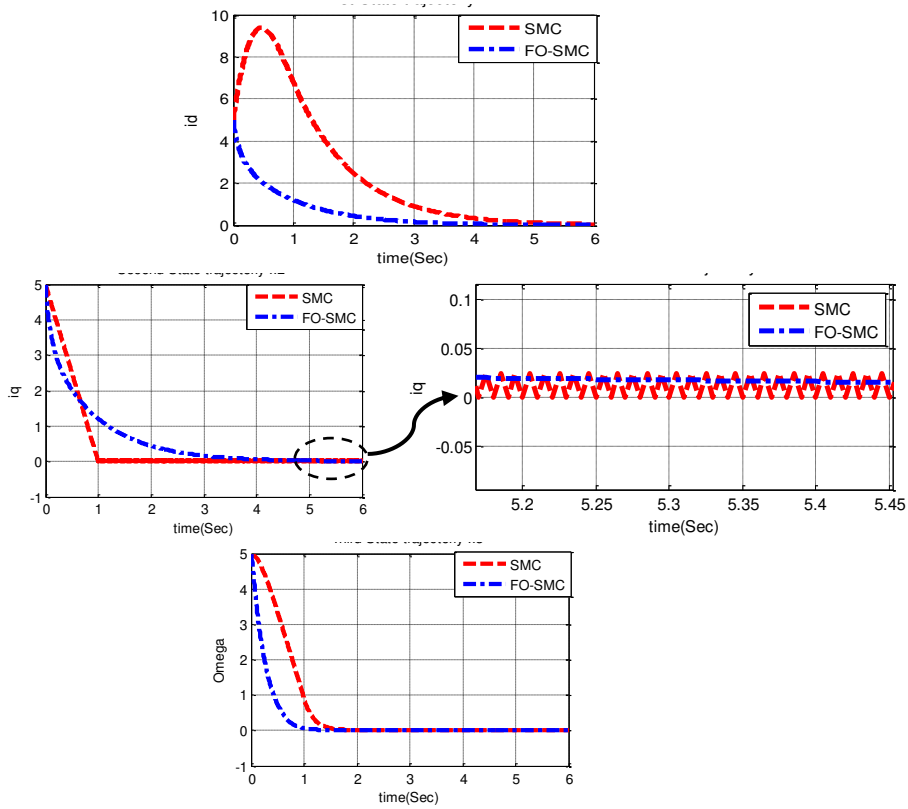


**Fig 7.** State trajectories regulation of $i_d$ , $i_q$ and Omega variables in fractional-order BLDC system using fractional-order sliding mode control signal.

Based on Fig 7, it can be observed that in the conventional sliding mode control strategy, the current $i_d$ experiences a large overshoot at the beginning of the time, which may lead the system to saturation. On the other hand, based on Fig 7, it can be seen that the current $i_q$ exhibits frequency oscillations over time in the conventional sliding mode control strategy, which lowers the system performance, while the proposed method is completely smooth.

As shown In Fig 8, the superiority of the proposed method is somewhat evident.

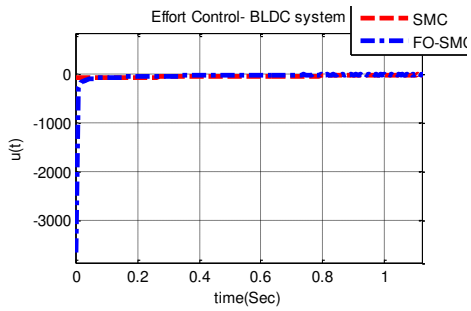


**Fig 8.** Control effort for state regulation of chaotic fractional-order BLDC system.

Based on Fig 8, it is evident that the proposed fractional-order sliding mode control strategy for fractional-order BLDC system requires much higher initial energy control, but this range limitation can be addressed by implementing a limiter if necessary.

Figure 9 illustrates the sliding surface used for state regulation of a chaotic fractional-order BLDC system. In this paper, the sliding surface is used to regulate the state of the BLDC system, which is known to exhibit chaotic behaviorunder certain conditions. By carefully designing the sliding surface, it is possible to control the system's dynamics and suppress chaotic behavior, leading to more predictable and stable operation. This is particularly important for practical applications of BLDC systems, where precise control over motor behavior is essential.

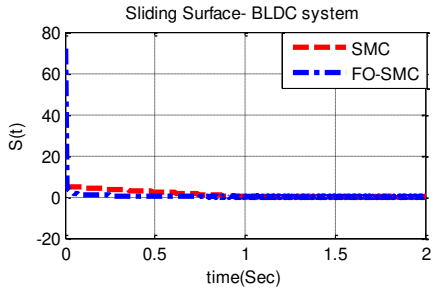


**Fig 9.** Sliding surface for state regulation of chaotic fractional-order BLDC system.

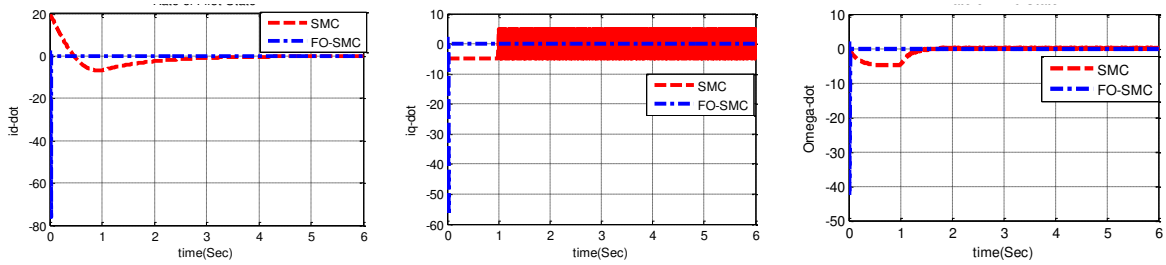


**Fig 10.** State rate trajectories regulation of variables $i_d$ , $i_q$ and Omega in fractional-order BLDC system using fractional-order sliding mode control signal.

In Fig. 10, which depicts the state rate trajectories of variable $i_q$, high frequency oscillations can be observed in the rate of change of the second state variable when using the sliding mode control method. However, this deficiency is not observed in the proposed method. The state rate trajectories of variable $i_q$ are important indicators of the behavior of the BLDC system, and the presence of high frequency oscillations can negatively impact the system's performance and stability. The proposed method appears to provide a more effective means of regulating the state rates, resulting in smoother and more stable behavior of the BLDC system.

To evaluate the performance of the controllers used in this paper, we use the following error metrics, which are the average sum of absolute errors:

$$\begin{cases} E_x = \frac{1}{T}\int_{T_0}^{T}(|e_{x_1}| + |e_{x_2}| + |e_{x_3}|)dt \\ E_{x-dot} = \frac{1}{T}\int_{T_0}^{T}(|e_{x_1-dot}| + |e_{x_2-dot}| + |e_{x_3-dot}|)dt \end{cases} \quad (33)$$

Where $e_{x_1} = x_{1d} - x_1$, $e_{x_1-dot} = \dot{x}_{1d} - \dot{x}_1$, and $T = T_s.t_f$.

In Table (1), which is presented for quantitative comparison of these two control methods, it can be observed by calculating the average sum of absolute errors that the state regulation errors are somewhat close to each other, but there is a significant difference in the rate of change of state regulation errors, indicating the advantage and value of the proposed fractional-order sliding mode control method.

Table 1. Average sum of absolute errors for state and rate of change of state regulation for fractional-order sliding mode control and conventional sliding mode control.

| Average sum of absolute errors. | State regulation error ($E_x$) | Rate of change of state regulation error ($E_{x-dot}$) |
|---|---|---|
| **SMC** | 3.5018 | 8.1595 |
| **FO-SMC** | 3.3964 | 0.1524 |

4.1.3. Comparison of fractional-order sliding mode control strategy with conventional sliding mode control after applying parameter uncertainties and external disturbances to the system.

The fractional-order BLDC system with uncertainties and external disturbances is represented by equation (32):

$$\begin{cases} {}_0D_t^{q_1} x_1 = -x_1 + x_2 x_3 \\ {}_0D_t^{q_2} x_2 = -x_2 - x_1 x_3 + \gamma x_3 + u(t) \\ \qquad\qquad +\Delta g(x_1, x_2, x_3) + d(t) \\ {}_0D_t^{q_3} x_3 = -\sigma(x_3 - x_2) \end{cases} \tag{34}$$

Where $\Delta g(x_1, x_2, x_3)$ refers to parameter uncertainties and $d(t)$ refers to external disturbances, and we aim to observe the behavior and resistance of the system in response to these changes by applying them as inputs to the system. Moreover, these sentences are considered as the following equations [31]:

$$\begin{cases} \Delta g(x_1, x_2, x_3) = 10.75 \sin(10x_1(t)) \cos(3x_2(t)) \cos(\pi x_3(t)) \\ d(t) = 5.25 \cos(2x_2(t)) + 8.5 \sin(3t) \end{cases} \tag{35}$$

Now, similar to before, we consider the parameter vector as $(\mu, \gamma, \sigma) = (1, 20, 5.46)$, the homogeneous orders of the system as $q_1 = q_2 = q_3 = 0.995$, and $T_{sim} = 6\,sec$. The time constant as $h = 0.005$, and the initial conditions as $(x_1(0), x_2(0), x_3(0)) = (5, 5, 5)$. A switching gain of $k = 5$ is used, and based on the sliding mode control input, relation (32) is designed using the sign function. Its implementation in MATLAB software is used to plot the state paths, the state change rate, the control input, and the sliding surface of the proposed method. A comparison is made with normal sliding mode control, which is naturally applied to the normal derivative system, to determine the advantages of the proposed method.

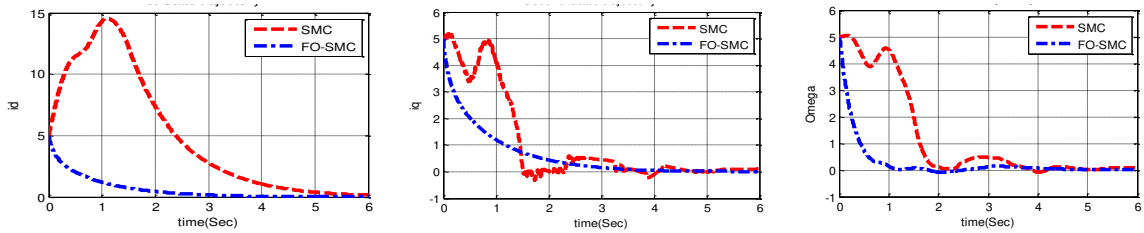


**Fig 11.** State trajectories regulation of $i_d$ , $i_q$ and Omega variables in fractional-order BLDC system using fractional-order sliding mode control signal in the presence of parameter uncertainties and external disturbances.

Observing Fig. 11, it becomes apparent that the conventional sliding mode strategy results in a significant overshoot in the current $i_d$ at the beginning of the time period, which may cause the system to become saturated. Additionally, it can be observed that the current $i_q$ in the conventional sliding mode strategy exhibits irregular, frequency-based oscillations over time, which reduces the system's overall performance quality. In contrast, the proposed method results in completely smooth behavior. Therefore, the performance of the proposed method is more desirable. Furthermore, the Omega plot indicates that the superiority of the proposed method is evident, as it exhibits better convergence speedand fewer oscillations.

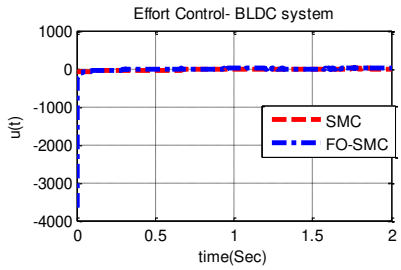


**Fig 12.** Effort for state regulation of fractional-order chaotic BLDC system in the presence of parameter uncertainties and external disturbances.

According to Fig 12, it is clear that the proposed fractional-order sliding mode control method for fractional-order BLDC system requires much higher initial energy for control, which, of course, imposes limitations on this method. However, if necessary, this limitation can be constrained by using a limiter on the energy.

Figure 13 shows the sliding surface used to regulate the state of a fractional-order chaotic BLDC system in the presence of parameter uncertainties and external disturbances. The sliding surface is a crucial component of control theory that helps stabilize system behavior under uncertain conditions. As can be seen in this Figure, the proposed method achieves negligible convergence time and convergence error, unlike the conventional sliding mode control method where the convergence of the sliding surface is undesirable. This highlights the superiority of the proposed method in providing more stable and predictable control of the BLDC system, even in the presence of parameter uncertainties and external disturbances.

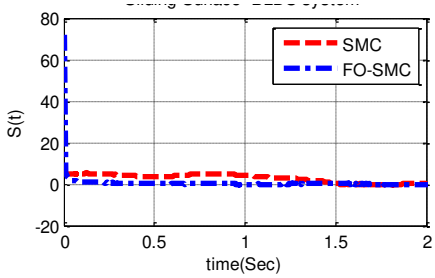


**Fig 13.** Sliding surface for state regulation of fractional-order chaotic BLDC system in the presence of parameter uncertainties and external disturbances.

Figure 14 illustrates the state rate trajectories of a BLDC system under the sliding mode control method and the proposed method. In the sliding mode control method, significant oscillations are observed in the rate of change of the first state variable ($i_d - dot$), which can negatively affect the current regulation of the system. However, this issue is not present in the proposed method. In addition, as shown in Figure 15, high-frequency oscillations and significant changes in the amplitude of the rate of change of the second state variable ($i_q - dot$) are generated under the sliding mode control method, which can be destructive for the current regulation of the system. However, these issues are not present in the proposed method. Furthermore, it can be observed that relatively high-amplitude oscillations with significant changes in the rate of change of the third state variable($\mathrm{Omega} - \mathrm{dot}$) over time are generated under the sliding mode control method, which can be destructive for the frequency regulation of the system. However, these issues are not present in the proposed method. These observations highlight the superiority of the proposed method in regulating the state rates of the BLDC system with smoother and more stable behavior compared to the sliding mode control method.

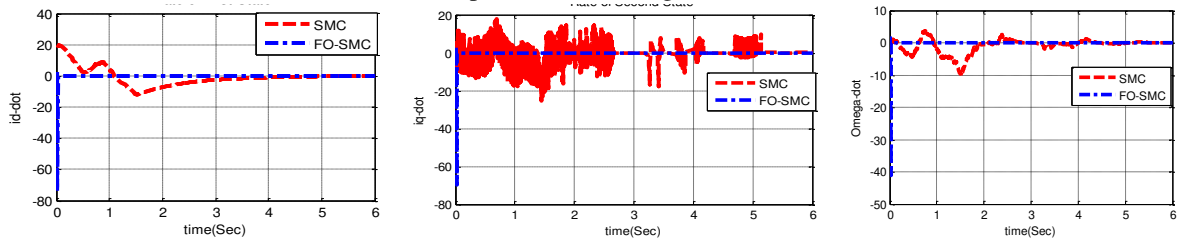


**Fig 14.** State rate trajectory regulation of variables $i_d$ , $i_q$ and Omega in fractional-order BLDC system using fractional-order sliding mode control signal in the presence of parameter uncertainties and external disturbances.

In Table 2, which is provided for quantitative comparison of these two control methods in the presence of parameter uncertainties and external disturbances, it can be observed that the average of the sum of absolute error values indicates a significant increase in the state regulation error in the conventional sliding mode control method compared to Table 1, while this increase is only at 0.05 in the proposed method. In the section of rate of change state regulation error, the state regulation error value in the conventional sliding mode control method has increased by one unit compared to Table 1, while this increase is only at 0.007 in the proposed method. This demonstrates the high advantage and resistance of the proposed fractional-order sliding mode control method compared to the desirable and robust conventional sliding mode method, which itself is a desirable and robust method compared to, for example, the PID method.

Table 2. Average sum of absolute errors for state and rate of change of state regulation for

fractional-order sliding mode control and conventional sliding mode control in the presence of parameter uncertainties and external disturbances

| Average sum of absolute errors. | State regulation error ($E_x$) | Rate of change of state regulation error ($E_{x-dot}$) |
|---|---|---|
| **SMC** | 7.2701 | 9.2106 |
| **FO-SMC** | 3.4487 | 0.1598 |

## 5. Conclusion

In this paper, a fractional-order sliding mode controller was designed to control a chaotic fractional-order system (chaotic BLDC system). For this purpose, by choosing an appropriate sliding surface and desirable input to the system, the design was made to control the chaotic behavior and bring it to the origin equilibrium point.

Sliding mode control is one of the most commonly used controllers for nonlinear systems and processes due to its relative simplicity and robustness against system uncertainties and external disturbances. The challenge in using this controller is the occurrence of chattering phenomenon on the sliding surface or chattering, especially in systems with fast dynamics. It was observed that with the help of sliding mode control, the system states converged to the required state in a limited time, but there were significant fluctuations in the system states, especially in the $x_1$and $x_{1-dot}$ states. To reduce this problem, fractional-order sliding mode control was used and applied to the fractional-order BLDC system, which made the behavior smoother and reduced the vibration of the system states. Moreover, it provided better adaptation of the control system and increased its resistance to uncertainties and external disturbances.

The qualitative (graphical representation) and quantitative (Tables 1 and 2) superiority between these two control strategies is justified by the authors for two important reasons:

- By converting the conventional system to a fractional-order system, as mentioned in previous sections, a fractional-order integration operation is first performed on the system, which reduces the existing error in the system.
- By using fractional-order control, which has a special innovation in this paper and that is the use of a linear continuous part alongside the relay control according to equation (30) in the switching control section, the control behavior is much smoother. As the advantages of fractional-order are used in the controller, the adaptation of the control system and the resistance to parameter uncertainties and external disturbances have also increased significantly.

## Conflict of interest

The authors declare that they have no conflict of interest.

## References

[1] Tang C, Bai L, Zhang G, Yang J, Li T (2020) Robust guaranteed cost control of PMSM chaotic system with uncertain parameters. Journal of Engineering Science and Technology Review, 13(3), 181-190. https://doi.org/10.25103/jestr.133.01

[2] Sun L X, Lu S, Wen ZG, Li YF (2019) Analysis of chaotic motion mechanism of permanent magnet synchronous motors. Electric Machines and Control, 23(3), 97-104. https://doi.org/10.16383/j.aemc.2019.3.001

[3] Zhou P, Cai H, Yang C D (2016) Stabilization of the unstable equilibrium points of the fractional-order BLDCM chaotic system in the sense of Lyapunov by a single-state variable. Nonlinear Dynamics, 84(4), 2357-2361. https://doi.org/10.1007/s11071-015-2452-2

[4] Jay P S, Binoy K R, Nikolay V K (2017) Multi stability and hidden attractors in the dynamics of permanent magnet synchronous motor. International Journal of Bifurcation and Chaos, 27(11), 1750159. https://doi.org/10.1142/S0218127417501596

[5] Wu S, Zhang JA (2018) Terminal sliding mode observer based robust backstepping sensorless speed control for interior permanent magnet synchronous motor. International Journal of Control, Automation and Systems, 16(6), 2743-2753. https://doi.org/10.1007/s12555-016-0782-x

[6] Petras I (2011) Fractional-order nonlinear systems: Modeling, analysis and simulation. Springer.

[7] Hilfer R (2000) Applications of fractional calculus in physics. World Scientific Pub. Co.

[8] Li S, Li P, Zheng Z, Zhang L (2023). Fractional order sliding mode control for circulating current suppressing of MMC. Electrical Engineering, 1-10. https://doi.org/10.1007/s00202-023-01902-7

[9] Qi G (2017) Energy cycle of brushless DC motor chaotic system. Applied Mathematical Modelling, 51, 686-697. https://doi.org/10.1016/j.apm.2017.06.001
[10] Kuroe Y, Hayashi S (1989) Analysis of bifurcation in power electronic induction motor drive systems. Proceedings of IEEE Power Electronics Specialists Conference, 923-930. https://doi.org/10.1109/PESC.1989.70573
[11] Li Z, Park J, Zhang B, Chen G (2002) Bifurcations and chaos in a permanent-magnet synchronous motor. IEEE Transactions on Circuits and Systems I, 49(3), 383-387. https://doi.org/10.1109/81.989966
[12] Xia C (2012) Permanent magnet brushless DC motor drives and controls. John Wiley & Sons Singapore Pte. Ltd.
[13] Jabbar M A, Phyu H N, Liu Z, Bi C (2004) Modeling and numerical simulation of a brushless permanent-magnet DC motor in dynamic conditions by time-stepping technique. IEEE Transactions on Industry Applications, 40(3), 763-770. https://doi.org/10.1109/TIA.2004.826330
[14] Hemati N (1994) Strange attractors in brushless DC motors. IEEE Transactions on Circuits and Systems I: Fundamental Theory and Applications, 41(1), 40-45. https://doi.org/10.1109/81.265867
[15] Lia C, Lia F, Li F (2014) Chaos induced in brushless DC motor via current time-delayed feedback. Optik, 125, 6589-6593. https://doi.org/10.1016/j.ijleo.2014.06.026
[16] Zaher A (2008) A nonlinear controller design for permanent magnet motors using a synchronization-based technique inspired from the Lorenz system. Chaos, 18, 013111. https://doi.org/10.1063/1.2837056
[17] Mohammad A, Arash K, Behzad G (2010) Control of chaos in permanent magnet synchronous motor by using optimal Lyapunov exponents placement. Physics Letters A, 374, 4226-4230. https://doi.org/10.1016/j.physleta.2010.09.073
[18] Ge Z, Lin G (2007) The complete, lag and anticipated synchronizationof a BLDCM chaotic system. Chaos, Solitons & Fractals, 34, 740-764. https://doi.org/10.1016/j.chaos.2006.05.057
[19] Ye S, Chau K T (2007) Chaoization of DC motors for industrial mixing. IEEE Transactions on Industrial Electronics, 54, 2024-2032. https://doi.org/10.1109/TIE.2007.903252
[20] Reyes R, Cruz C, Nakano-Miyatake M, Perez-Meana H (2010) Digital video watermarking in DWT domain using chaotic mixtures. IEEE Latin America Transactions, 8, 304-310. https://doi.org/10.1109/TLA.2010.5438444
[21] Chau KT, Wang Z (2011) Chaos in Electric Drive Systems—Analysis, Control and Application. John Wiley & Sons (Asia) Pte Ltd., Singapore. https://doi.org/10.1002/9781118098199
[22] Roy P, Ray S, Bhattacharya S (2014) Control of Chaos in Brushless DC Motor Design of Adaptive Controller Following Back-Stepping Method. In: International Conference on Control, Instrumentation, Energy & Communication (CIEC). https://doi.org/10.1109/CIEC.2014.107
[23] Patra A, Chakrabarty K, Nag T (2018) Control of Chaos in BLDC Motor Drive. In: Proceedings of IEEE, Applied Signal Processing Conference (ASPCON). https://doi.org/10.1109/ASPCON.2018.8605733 Yaz M,
[24] Cetin E (2021) Brushless Direct Current Motor Design and Analysis. COJ Electronics & Communications. https://doi.org/10.31031/COJEC.2021.05.000602
[25] Rajagopal K, Vaidhyanathan S, Karthikeyan A, Duraisamy P (2016) Dynamic Analysis and Chaos Suppression in a Fractional Order Brushless DC Motor. Springer. https://doi.org/10.1007/978-3-319-32273-5_2
[26] Xue G, Lin F, Qin B (2020) Adaptive Neural Network Control of Chaotic Fractional Order Permanent Magnet Synchronous Motors Using Backstepping Technique. Frontiers in Physics. https://doi.org/10.3389/fphy.2020.00062
[27] Zhou P, Bai R, Zheng JM (2015) Stabilization of a Fractional-Order Chaotic Brushless DC Motor via a Single Input. Springer.
[28] DeCarlo RA, Zak SH, Matthews GP (1988) Variable Structure Control of Nonlinear Multivariable Systems: A Tutorial. Proceedings of the IEEE 76(3):212-232. https://doi.org/10.1109/5.2070
[29] Utkin VI (1992) Sliding Modes in Control and Optimization. Springer.
[30] Hung JY, Gao W, Hung JC (1993) Variable Structure Control: A Survey. Proceedings of the IEEE 40(1):2-20. https://doi.org/10.1109/5.210201
[31] Shahzad M (2016) Chaos Control in Three Dimensional Cancer Model by State Space Exact Linearization Based on Lie Algebra. International Journal of Engineering & Technology 4(33):1-11. https://doi.org/10.14419/ijet.v4i3.6129